

Focal Scanning for Optical Detection of Radiation

Oskar F Searfus, University of New Mexico

B.S. Nuclear Engineering, Expected May 2020

Manager Steve Vigil, Mentor Jeff Martin, Org. 6752

Presented July 24, 2019

Abstract:

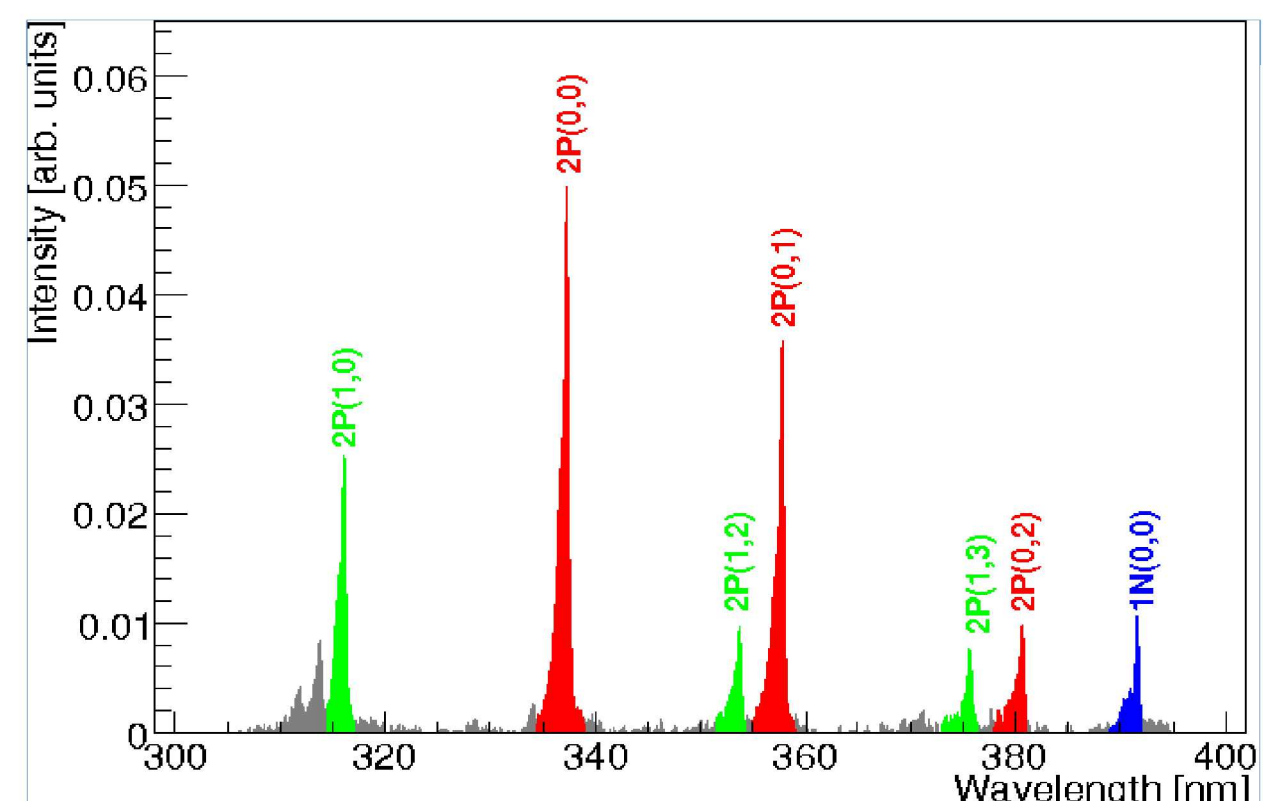
Detection of ionizing radiation is possible via the collection of ultraviolet (UV) photons emitted by the deexcitation of nitrogen molecules present in air excited by charged particles. Modern cameras and geometric optics are able to image this UV signal, and provide a map of radiation dose in air. However, a single image integrates all signal, in and out of focus, along the axis normal to the lens of the camera, and cannot determine the radioactive source position along this axis. In this experiment, the focal length of the camera lens was “scanned” in order to determine the source position.

Introduction:

Optical Detection of Radiation (ODR) generally refers to the use of optical equipment to collect fluorescence photons produced by the deexcitation of molecules and atoms in air, primarily nitrogen (N_2) in the scope of this report. When charged particles associated with ionizing radiation collide with a nitrogen molecule, electrons in the molecule may be ejected or excited (Turner, 1995), and when the electrons return to their ground state, photons are emitted in several bands of the ultraviolet (UV) spectrum. The photons produced by the absorption of radiation are unique: deexcitation of N_2^+ ions produces photons distinguishable from the deexcitation of neutral N_2 molecules. The principal electromagnetic spectral bands for the purposes of this report are at 316, 337, 358, and 391 nm, the most intense of which being 337 nm (Belz, 2006). However, relatively few UV photons are produced by radiation dose deposited in air; consequently, equipment used for their collection must be highly sensitive, and methods must be devised to reduce background signal as much as possible to maximize the utility of ODR results. Using modern UV sensitive cameras and optical equipment, it is possible to produce an image of the dose field associated with a radioactive source.

Alpha radiation is of primary interest for ODR. Due to its high specific ionization and short range, it produces a minimum interaction volume in which it deposits its energy, and out-of-focus signal contribution is minimized when compared to beta, gamma, and neutron radiation.

A prominent application for ODR is to determine the presence and location of unknown sources from a remote distance, particularly alpha radiation, which has a range of only a few centimeters and traditionally cannot be detected outside of this range (Knoll, 2010). This may be done for environmental diagnostics in the field of radioactive material cleanup, uranium ore identification, etc. ODR has also been utilized for millennia as a familiar visible phenomenon in ultra-high energy cosmic ray astronomy: As the earth's magnetic fields concentrate cosmic rays and solar winds toward the earth's poles, fluorescence of the air, caused by radiation, can be seen with the naked eye in the natural occurrence known as aurora. With further development, ODR may be used to replace diagnostic thermoluminescent dosimeters (TLD) in pulsed power radiation facilities and medical radiation imaging facilities, as detailed dose mapping may be viable. Large arrays of TLDs can be costly and only give discrete dose information, so the photographic nature of ODR may be able to give more detailed dose information at a lower cost.



Nitrogen Rad-induced Fluorescence bands in the UV regime (Waldenmaier 2008)

Data Collection and Analysis Methodology:

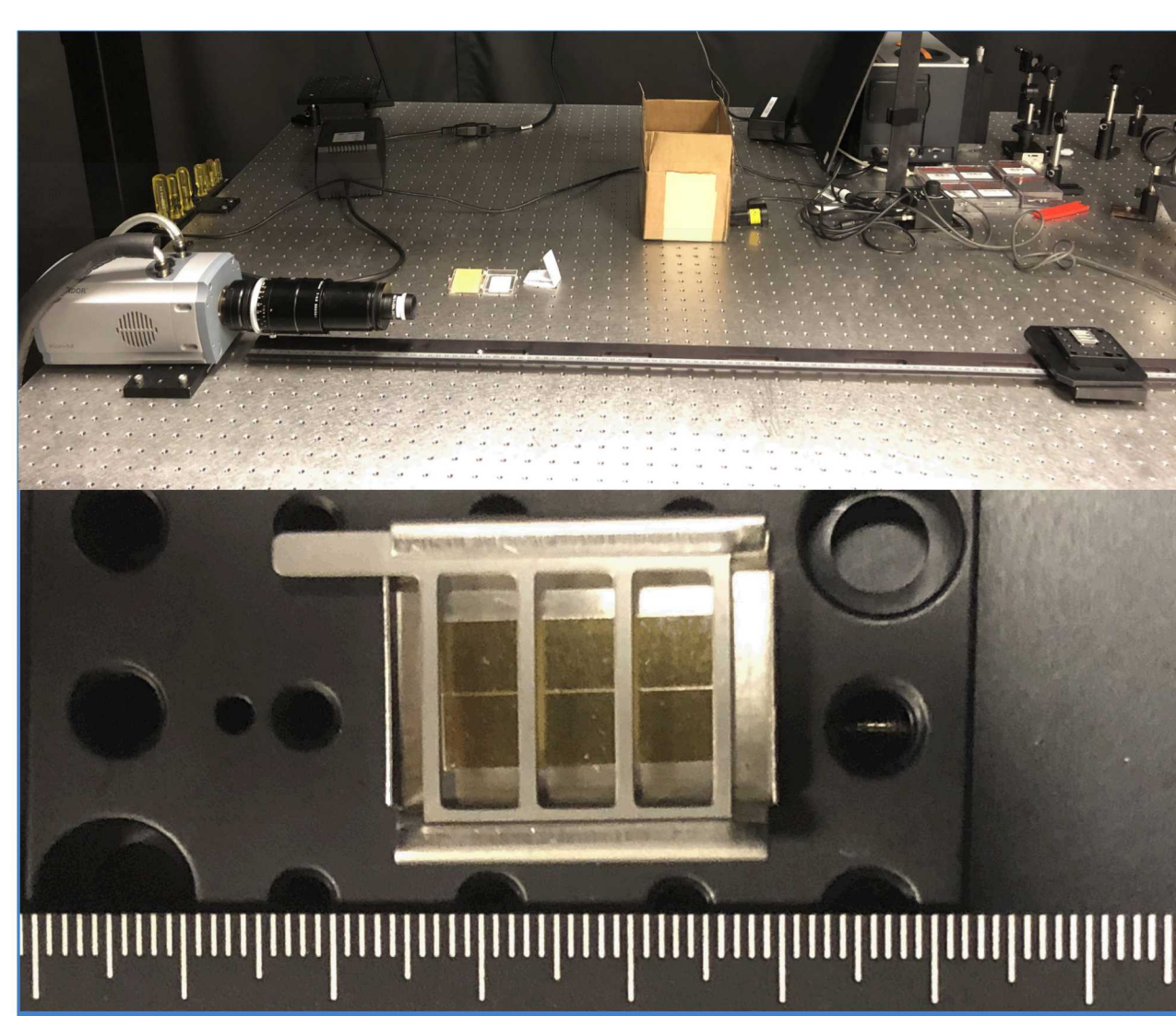
Measurements in this experiment were carried out exclusively using the Andor iKON iCCD camera, Nikkor 105mm UV lens, and a custom Sandia-made dual band (340 and 360 nm) filter. For general signal characterization, a 365 nm UV LED was used as a surrogate for radiation-induced signal, to aid in timeliness in data collection. Radiation signals were produced by two alpha radiation sources: a 40 mCi “can” source, and a 500 μ Ci “stamp” source, both ^{210}Po . The stronger can source consists of an aluminum tube, with two polonium-containing plates adhered to its interior, opposite each other. On either end of the tube, wide aluminum mesh exists to prevent disturbance of the active regions within. The weaker stamp source consists of a small aluminum tray with a small polonium-containing plate adhered within. There are two aluminum bars above the active region.

Measurements of the LED and the radiation sources were carried out on an optics table, with the LED or source placed a fixed distance from the camera. Images were collected at various preset focal lengths as set on the lens, scanning from “in front” of the source to behind it. When the LED was imaged, short acquisition times (10 ms) were utilized due to its intense nature, and when the radioactive sources were imaged, much longer acquisition times (~ 30 min) were required to measure enough photons for a quality image.

Images from this apparatus were then processed in MATLAB to extract meaningful information and determine the source position. The data analysis script written determines a small background region, and subtracts the average pixel value of this region from the entire image. Then, a gaussian image filter is applied to the image to reduce the impact of “hot” pixels which become prominent in long exposures, created by cosmic rays and background gamma radiation incident on the camera sensor. The script then bins each pixel into “signal” and “background” matrices, with signal pixels determined to be such if their value is greater than three standard deviations of the original background mentioned previously (unfiltered). The total signal above background is then calculated, and divided by the number of signal pixels to determine average signal value. Signal-to-Noise ratios (SNR) for each image are then calculated by

$$SNR = \frac{\text{Average Signal}}{\sigma_{bkg}}$$

Where σ_{bkg} is the standard deviation of the complete background bin (i.e., all pixels not binned as signal).

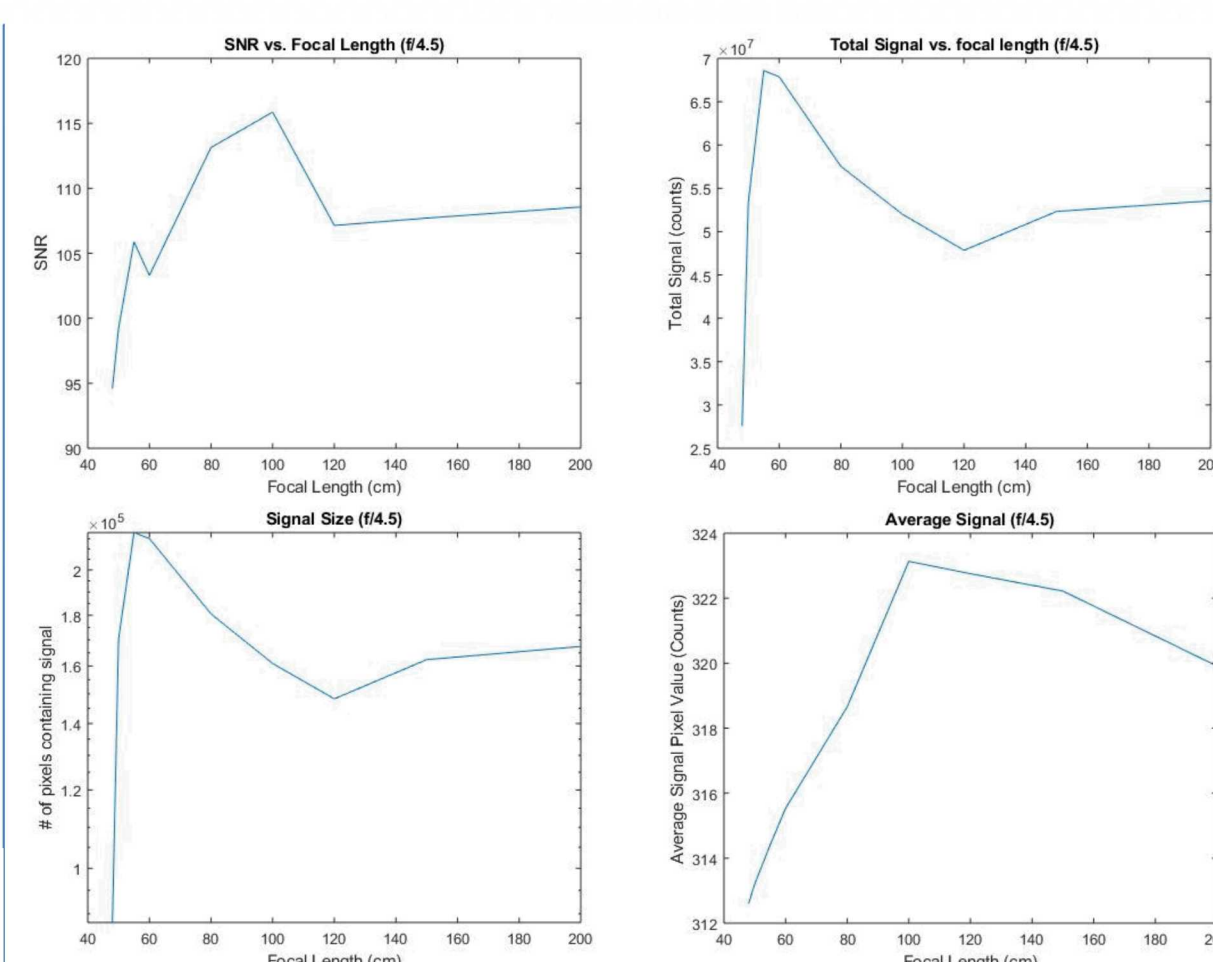


Sample test set-up, showing the 500 μ Ci “stamp” Po-210 Source

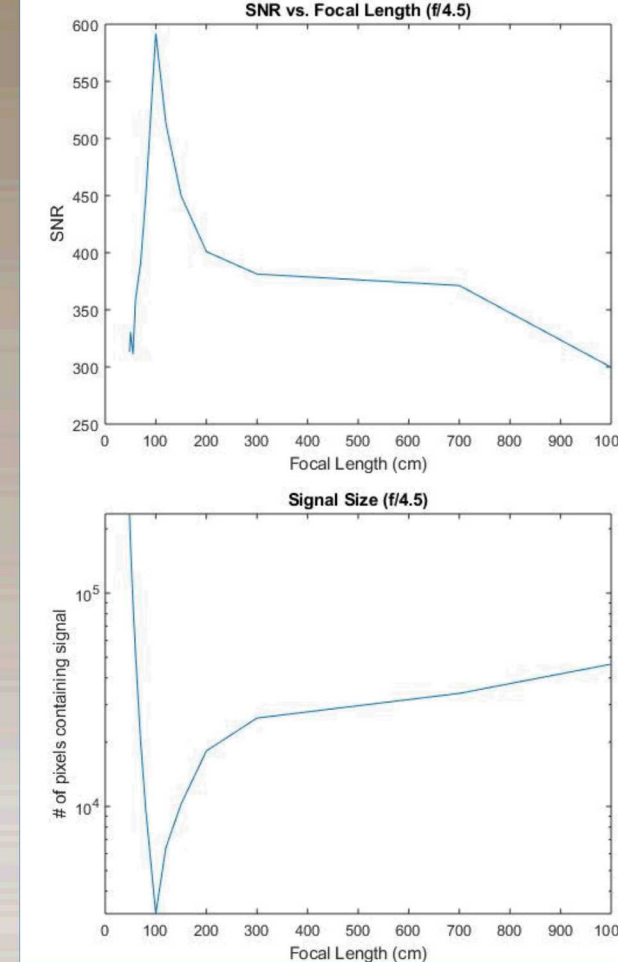
Results:

In LED images taken and processed as described previously, a clear peak in SNR is observed when the focal length is set at the position of the source. Some other interesting phenomena were also observed in the intermediate steps of data processing pertaining to the size and total strength of signal as a function of focal length. The total signal, i.e. the sum of all background-subtracted signal pixels, is minimized when the focal length is the same as the source location. The signal size, i.e. the total number of pixels containing signal, is also minimized when the focal length is the same as the source location as expected, however, the trend it follows is extremely different on either side of this minimum.

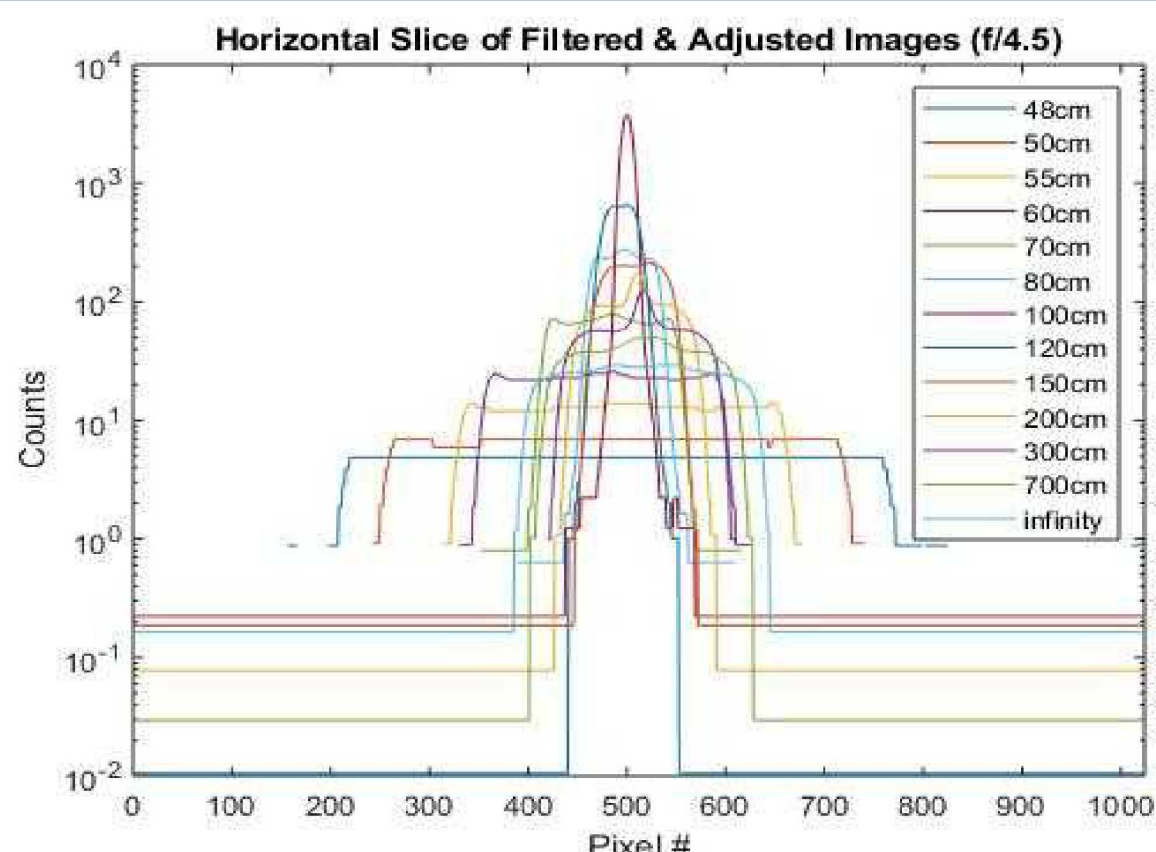
Several challenges became apparent when imaging actual radiation-induced images, particularly in data processing. The long acquisition times required to capture an adequate image of such a low signal means that significant quantities of cosmic rays and gamma radiation (803 keV emitted in 0.001% of Po-210 decays) are incident on the camera sensor, and hot pixels must be mitigated as a result. Even with mitigation, the standard deviation of the background is much greater and more variable from image to image in radiation images than in LED images. The radiation-induced signal is also significantly more distributed than the LED signal (the range of 5.3 MeV alphas in Albuquerque air is approximately 5 cm), such that the average signal value is much lower. These factors lead to an overall decrease in SNR, and the inconsistent background noise produces a much less smooth SNR function than with LED images. Average signal value alone, however, can potentially be enough to determine the source location.



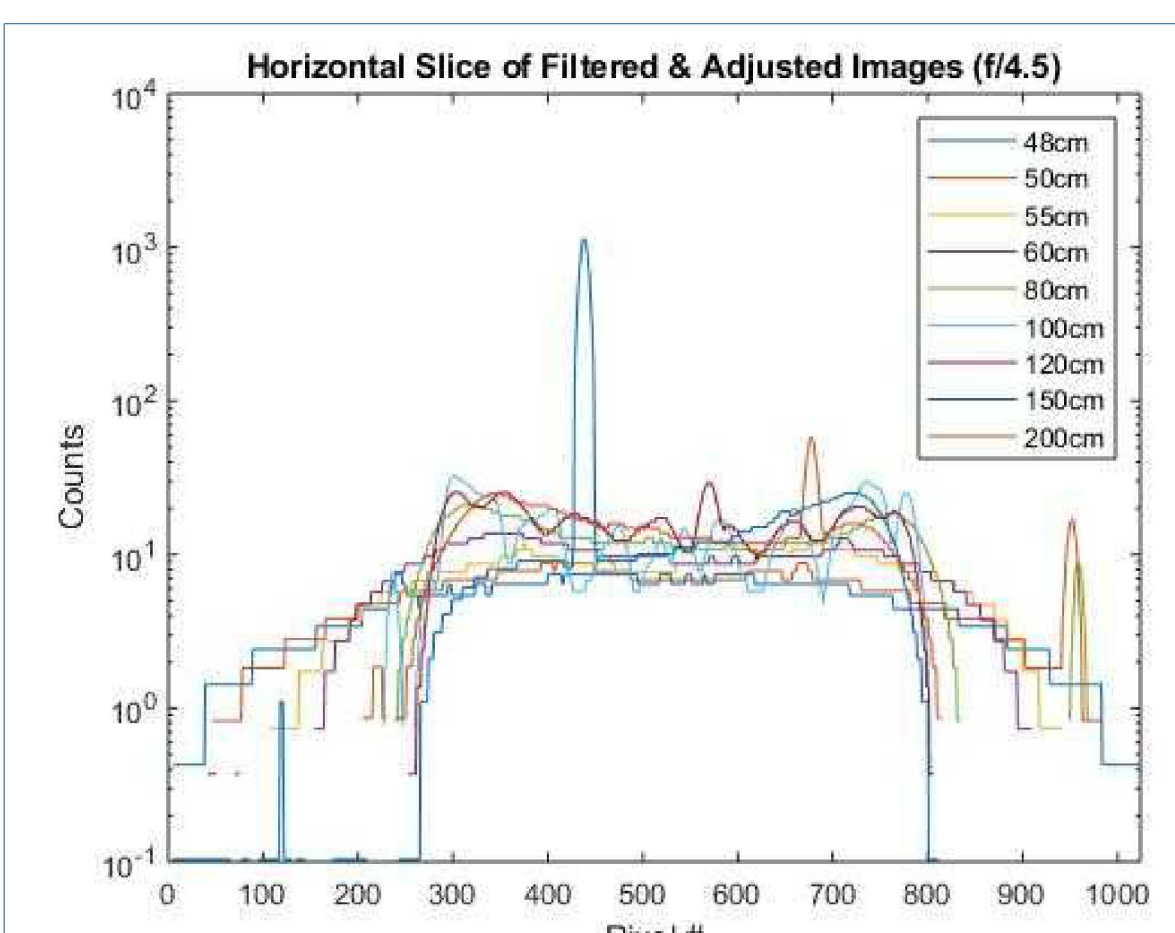
Sample Results from LED Images



Sample Results from Po-210 "can" Images



Cross-sectional slices of LED images at varying focal lengths



Cross-sectional slices of Po-210 "can" images at varying focal lengths

Discussion and Further Work:

These tests clearly demonstrated the feasibility of ODR for location of alpha-emitting radioactive material from a remote distance, far greater than the range of alpha particles and traditional detection limits. Beyond lateral location in the field of view, as demonstrated in many previous works, this method also permits the location of radioactive material along the axis of the camera lens. As shown in this experiment, there are multiple foci that could lead to the same SNR with the same radioactive source, leading to a large uncertainty in position in the case that only a single image is taken. Even without a quantitative processing algorithm, qualitative visual comparisons of images at varying focal lengths permits largely accurate estimations of source location.

There is much room for improvements from these measurements, however. Improved shielding of the camera against gamma radiation and cosmic rays would likely significantly improve SNR calculations in long-exposure radioactive source measurements, and would be necessary if this technique were to be fielded in a mixed-radiation field where gamma rays are more abundant.

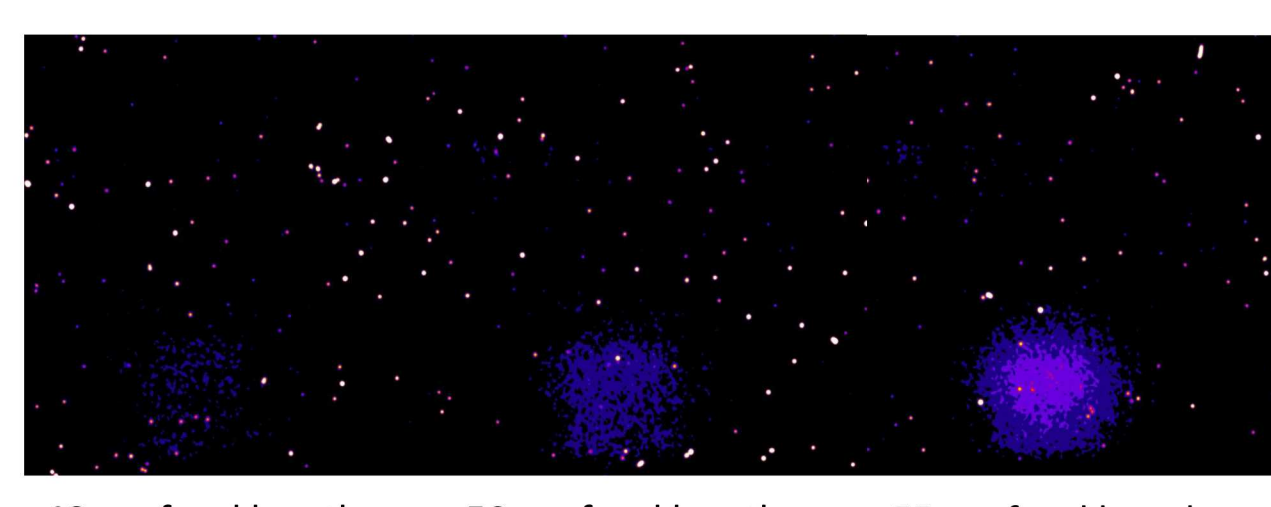
Furthermore, these measurements should be repeated with comparably strong beta radiation sources, as beta radiation has a significantly greater range than alpha radiation does. This will likely broaden the SNR peak, and require a larger range of focal lengths to make an accurate estimate of position.

Acknowledgments:

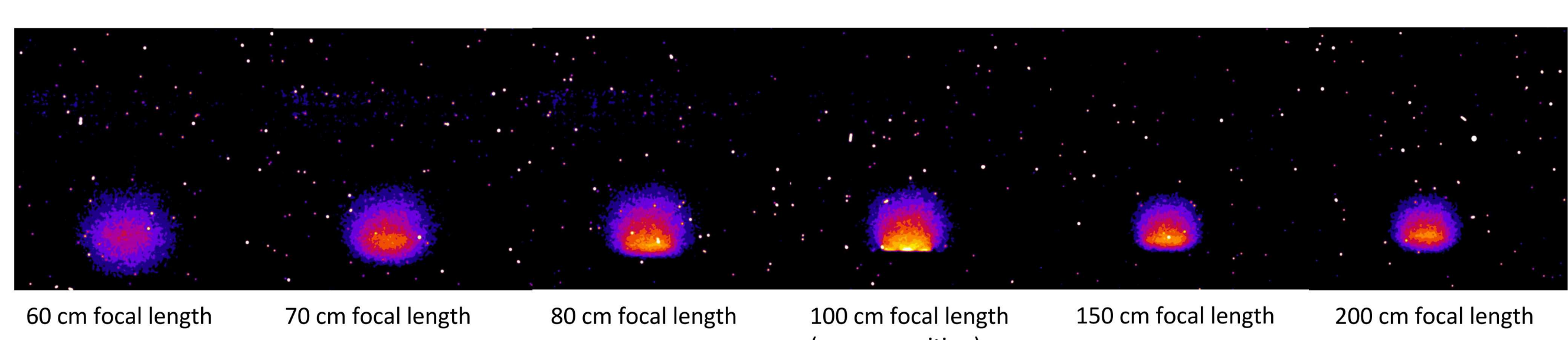
This work would not have been possible without the assistance of Jeff Martin and Rick Harrison. Their patient and insightful support guided me through this research, and they are responsible for introducing me to the field of Optical Detection of Radiation.

References:

- Belz, J. (2006). Measurement of Pressure Dependent Fluorescence Yield of Air: Calibration Factor for UHECR Detectors. *Astroparticle Physics*, 129-139.
- Knoll, G. (2010). *Radiation Detection and Measurement*. Ann Arbor, MI: Wiley and Sons.
- Turner, J. E. (1995). *Atoms, Radiation, and Radiation Protection* (2nd ed.). New York, NY: John Wiley & Sons.
- Waldenmaier, T., Blumer, J., & Klages, H. (2008). Spectral Resolved Measurement of the Nitrogen fluorescence Emissions in Air Induced by Electrons. *Astroparticle Physics*, 205-222.



48 cm focal length 50 cm focal length 55 cm focal length



60 cm focal length 70 cm focal length 80 cm focal length 100 cm focal length 150 cm focal length 200 cm focal length (source position)